CLM-P54

United Kingdom Atomic Energy Authority

RESEARCH GROUP

Preprint

A STUDY OF HELICON WAVES IN INDIUM

G. N. HARDING
P. C. THONEMANN

Culham Laboratory,

Culham, Abingdon, Berkshire

1964

A STUDY OF HELICON WAVES IN INDIUM

by

G.N. HARDING
P.C. THONEMANN

A B S T R A C T

Measurements have been made of the phase velocity and the attenuation of helicon waves propagated parallel to the axis of a long cylinder of indium metal at 4.2^{o}K. A constant magnetic field was applied parallel to the axis of the cylinder. Both the axisymmetric (m = o) and dipole (m = ± 1) modes were studied.

The experimental results are compared with the predictions of theory for two different assumptions concerning the boundary conditions. It is shown that the theoretical predictions which involve surface currents and vacuum fields give the best agreement with the experiment.

The Hall coefficient derived from these measurements is consistent with that calculated on the assumption of one hole per atom within the experimental error (~1.5%).

J.K.A.E.A. Research Group,
Culham Laboratory,
Nr. Abingdon,
Berks.

August, 1964 (C/18 ED)

C O N T E N T S

1. INTRODUCTION

Helicons are circularly polarised electromagnetic waves which can be propagated under certain conditions through electrically conducting media in magnetic fields. These conditions are: (1) the wave frequency is less than the electron cyclotron frequency; (2) the collision frequency is less than the electron cyclotron frequency; they can be satisfied in the laboratory in three different kinds of medium, (a) gas discharge plasmas, (b) semiconductors, (c) very pure metals at low temperature.

The possibility of propagating the waves in suitable semiconductors was first pointed out by Aigrain (1960) who suggested the name "Helicon", and gave their main properties. They were demonstrated experimentally in very pure indium antimonide at $77^{o}K$ by Libchaber and Veilex (1962a, 1962b), who confirmed the predictions of Aigrain. Bowers, Legendy and Rose (1961) found similar waves using very pure sodium at $4.2^{o}K$, examined the properties of the waves in several metals, and used them to study the damping of cyclotron resonance, (Rose, Taylor and Bowers, 1962, Taylor, Merrill and Bowers, 1963a, 1963, Merrill, Taylor and Goodman, 1963). Cotti, Wyder and Quattropani (1962, 1963) observed the effect in indium and used it to obtain the Hall coefficient. Jones and Chambers (1962) carried out precise measurements of the resonant frequencies of standing helicon waves in thin rectangular samples and deduced values for the Hall coefficient of sodium, potassium, lithium, indium and aluminium.

In gaseous plasmas these waves are well-known in the earth's exosphere as "whistlers" (Storey, 1953). They have also been observed in laboratory plasmas by Gallet et al. (1960) and Dellis and Weaver (1964).

The present study was undertaken in parallel with a theoretical investigation of the properties of the waves in a bounded cylindrical medium by Klozenberg, McNamara and Thonemann (1964) referred to hereafter as KMT, and an experimental study of their propagation in a dense laboratory Xenon plasma (J. Lehane, private communication). The objects of the present experiments were: to find the dispersion relation by a method in which wavelength was measured directly and not inferred from the dimensions of a resonating sample; to measure attenuation in such a way that the results could be readily compared with theory, and to compare the experimental results with those calculated making different assumptions about the boundary conditions.

2. THE THEORY OF HELICONS IN A CYLINDRICAL MEDIUM

A detailed analysis of the propagation of helicon waves in a cylindrical medium has been given by KMT. Only the essential elements of this theory will be summarised here.

If $\underline{E}$ and $\underline{j}$ are the electric field and current density due to the wave and if the current is carried by electrons, the linearised equation connecting $\underline{E}$ and $\underline{j}$ is

$$\underline{E} - \frac{\underline{j} \times \underline{B}}{ne} - \eta \underline{j} = 0 \qquad \ldots (1)$$

where $\underline{B}$ is the applied uniform magnetic field in the direction of the cylinder axis, η the resistivity, n the electron density and e the proton charge. In Indium the current is carried by positive holes, and the sign in front of the second term of (1) would be positive in this case. However, it is convenient to discuss the theory for the case of electrons, the only difference for holes being that in the case of $m = 1$ waves, either the magnetic field or the sense of rotation of the wave must be reversed before comparison with the electron theory.

The second and third terms in equation (1) represent the electric fields due to the Hall effect and ohmic resistance respectively. For wave propagation to take place without excessive attenuation it is necessary that $\underline{j} \times \underline{B} \gg ne\eta\underline{j}$ or more simply $\Omega\tau \gg 1$, where Ω is the gyrofrequency of an electron in the magnetic field $\underline{B}$ and τ is the time interval between collisions. The motion of the lattice is neglected and the resistivity taken to be isotropic. Assuming a solution for the wave magnetic field of the form

$$\underline{b} = \hat{\underline{b}} e^{i(kz - \omega t + m\theta)}$$

and using the equations

$$\nabla \cdot \underline{b} = 0 \quad , \quad \nabla \cdot \underline{j} = 0$$

$$\nabla \times \underline{b} = \mu_0 \underline{j} \quad , \quad \nabla \times \underline{E} = -\frac{\partial \underline{b}}{\partial t} \quad ,$$

equation (1) may be written

$$i\mu_0 \omega \underline{b} - \frac{ikB}{ne} \nabla \times \underline{b} - \eta \nabla \times \nabla \times \underline{b} = 0 \qquad \ldots (2)$$

The general solution of (2) is the sum of the solutions of

$$\nabla^2 \underline{b} = -\beta_1^2 \underline{b} \quad \text{and} \quad \nabla^2 \underline{b} = \beta_2^2 \underline{b} \qquad \ldots (3)$$

where β_1 and β_2 are the roots of the equation

$$\mu_0 \omega - i\eta\beta^2 + \frac{Bk}{ne}\beta = 0 \, . \qquad \ldots (4)$$

The solutions of equations (3) in cylindrical co-ordinates are Bessel functions and since the wave fields must be finite at the origin, the solution for the fields contains

two arbitrary constants. Thus

$$b_z = A_1 J_m(r\,\beta_1^2 - k^2) + A_1 J_m(r\,\beta_2^2 - k^2) \qquad \ldots (5)$$

where J_m are Bessel functions of the first kind and A_1 and A_2 are arbitrary constants. Expressions for the b_r and b_θ components of the wave fields are given by KMT in terms of b_z.

Since resistivity has been included the wave fields are continuous across the plasma vacuum interface. The vacuum field components are given by

$$\underline{b} = \nabla\varphi \quad \text{where} \quad \nabla^2\varphi = 0 \qquad \ldots (6)$$

In general the solution for the vacuum field involves two arbitrary constants. However, this field must vanish at infinity and one constant must be zero. Matching of the plasma field and the vacuum field components at the boundary ($r = a$) yields three equations involving three arbitrary constants which may be eliminated to yield the dispersion relation. This procedure is different from that of Bowers et al (1961) and Cotti et al (1962, 1963) who assumed that the normal component of the wave field vanished at the boundary of a rectangular prism and therefore there were no vacuum fields. Jones and Chambers (1962) pointed out that the dispersion relation used by Bowers et al. and by Cotti et al. was strictly true only for an infinite medium, but concluded that the component of the wave vector perpendicular to the surface of a thin rectangular plate of thickness a, orientated normal to the applied magnetic field, was given by $k_z = n\pi a$ with negligible error, provided the width in both directions normal to the applied field greatly exceeded the thickness a. To illustrate the order of the error following the assumption that the vacuum magnetic field is zero, the dispersion relation obtained by assuming that $b_r = 0$ at $r = a$ has also been calculated and is compared with that for $b_r \neq 0$ at $r = a$ and with experimental results.

The dispersion relation for the case $b_r \neq 0$ at $r = a$ and for $m = 0$ is

$$\begin{vmatrix} \frac{k}{\gamma_1} J_1(a\gamma_1) & \frac{k}{\gamma_2} J_1(a\gamma_2) & ikK_1(ak) \\ \frac{\beta_1}{\gamma_1} J_1(a\gamma_1) & \frac{\beta_2}{\gamma_2} J_1(a\gamma_2) & 0 \\ J_0(a\gamma_1) & J_0(a\gamma_2) & k\,K_0(ak) \end{vmatrix} = 0$$

where $\gamma^2 = \beta^2 - k^2$ and K_1, K_0 are modified Bessel functions of the second kind.

Apart from giving a different wavelength frequency relation compared to the case of no vacuum field the KMT theory predicts an enhanced wave attenuation due to surface currents. The measured attenuation is compared with the theoretical predictions in section 4.

3. EXPERIMENTAL ARRANGEMENT

The general arrangement used for the measurements is shown in Fig.1. The sample in the form of a circular cylinder, 0.8 cm in diameter and 9.4 cm long, was placed in a cryostat with a magnetic field parallel to its axis. Waves were launched continuously at one end by an arrangement of coils, and detected by other coils which could be moved along the sample by means of an external micrometer screw. By measuring the phase and amplitude of the detected signal the wavelength and attenuation of the waves was found. Of the many modes possible in a cylinder, two were studied, the axi-symmetric m = o, and that having a single diametral axis of symmetry m = ± 1. These correspond roughly to the TE01 and TE11 modes in circular waveguides. For the m = ± 1 modes, the positive sign corresponds to the case when the rotation of the wave pattern is in the same sense as the rotation of the holes in the applied magnetic field.

The metal chosen for this investigation was indium, because of its high conductivity and low magnetoresistance. In some preliminary experiments highly purified sodium was used, but the need to protect it from the atmosphere gave rise to difficulties in the design of the experiment which were eliminated by working with indium. The indium used* contained less than 0.4 p.p.m. impurity, and at 4.2^{o}K in a magnetic field of 15 kg had a value for $\Omega\tau$ of about 20. This gave a damping length (distance for the field to fall to 1/e) of the order of 1 cm, a value allowing both wavelength and absorption coefficient to be measured with considerable accuracy (see below).

The indium rod was made by extruding the vacuum-cast material through a die. The magnetic field was provided by a superconducting solenoid wound with Nb-Zr wire, giving a magnetic field of up to 15.4 kilogauss with a uniformity better than 1% over a region 4 cm long and 1.3 cm in diameter. The measurements were all made within this region, but the specimen was continued into the region of lower field at one end of the solenoid in order to increase damping of the waves and prevent reflection from the end of the sample. In this way only waves travelling in one direction were detected, and the measurements were not complicated by standing waves.

---

* "6N grade" obtained from Koch-Light Laboratories, Colnbrook.

For the m = o mode, the launching coil, of mean diameter 6 mm and length 1 mm, and having 100 turns of 45 s.w.g. wire, was placed 0.5 mm from the (flat) end of the indium rod. It energised the axial component of the vacuum magnetic field associated with the wave, which has a maximum value on the axis. The receiving coil arrangement was designed to detect the radial component of the vacuum field outside the sample and consisted of two similar coils, connected so that any current induced in them by axial magnetic field components would cancel. In this way currents induced directly from the launch coil were minimised. The receiving coils, each with 200 turns of 45 s.w.g. wire, mean diameter 10.5 mm, and length 0.5 mm, had a gap of 0.5 mm between them. Direct pickup between the launch and receiving coils was further reduced by massive copper shielding.

For the m = 1 mode two rectangular coils with axes perpendicular to one another and to the axis of the sample were fed with driving currents having a $\pi/2$ phase difference. This gave a rotating magnetic field pattern which energised both radial and azimuthal components of the vacuum field. Two rectangular receiving coils 4 mm × 4 mm were placed on opposite sides of the sample, their axis perpendicular to the axis of the sample, and slightly bent to fit a cylindrical support.

The frequency range covered in the experiments was from 1 - 100 c/s and the corresponding wavelength range was from 4.5 cm to 0.4 cm.

After amplification, the received signals were displayed on a calibrated double-beam oscilloscope, together with a reference signal in phase with the launching current. The receiving coils were moved, usually in 1 mm steps, and the amplitude and relative phase measured.

The magnetic field was measured by nuclear magnetic resonance technique, using ^{19}F nuclei in coloured fluorite. The low-frequency oscillator used to launch the waves was calibrated against a 50 c/s valve-maintained tuning fork, the accuracy of which was better than 1 part in 10^4.

4. MEASUREMENTS AND RESULTS

In Figs. 2 and 3 are shown the results of measurements of phase and amplitude as the receiving coil was moved along the sample. The measurements were at 50 c/s where the accuracy was high and embraced seven wavelengths and an attenuation of 13:1. The wavelengths and attenuation were determined from the slopes of straight lines drawn through the points in plots similar to Figs. 2 and 3. The small amount of direct pickup between

the transmitting and receiving coils, determined by (a) removing the magnetic field and (b) removing the sample, was subtracted electrically by means of a compensating circuit.

Most of the measurements were made at the maximum value of magnetic field possible with the superconducting solenoid (15.4 kg). The experimental points of the wavelength and attenuation measurements at a constant magnetic field of this value are shown in Figs. 4 and 5 (m = o) and 6 and 7 (m = 1). For comparison with the theory, the wavelength and attenuation are converted into the dimensionless quantities $ak_r = 2\pi a/\lambda$ (where a is the radius of the sample and λ the wavelength measured along the axis) and ak_i = radius/damping length, where $k = k_r + ik_i$. The frequencies are plotted as ω/ω_o where ω is the angular frequency and $\omega_o = B/\mu_o nea^2$.

Experiments in which the magnetic field was varied while the frequency was kept constant gave dispersion relations agreeing within the experimental error with those obtained by varying the frequency and keeping the magnetic field constant.

On Figs. 4 - 7 are also plotted the computed dispersion relations and variation of attenuation with frequency for various values or $\Omega\tau$, both from the KMT theory and using boundary conditions such that there are no vacuum fields and no surface currents, as discussed in Section 2 above. In order to find the value of ω_o needed for plotting these curves, the density of the indium was measured at 20°C and found to be 7.29_0. This gives a Hall coefficient at 4.2°K of 1.600×10^{-4} cm^3 amp^{-1} sec^{-1}, using Swenson's (1955) value of 0.71% for the linear contraction of indium between 20°C and 4.2°K, and assuming that there is one hole per atom. On the Figures showing the attenuation results, the curves computed using the KMT theory are labelled "surface and volume damping" because of the enhanced attenuation due to surface currents, and those with the b_r = o boundary conditions are labelled "volume damping only".

In another series of measurements, the parameter $\Omega\tau$, and therefore the attenuation, was varied by changing the magnetic field, while ω/ω_o, and hence the wavelength, was held constant by keeping the ratio of frequency to magnetic field constant. The results are shown in Figs. 8 and 9, where the quantities plotted are ak_i vs. $1/\Omega\tau$. The values of $\Omega\tau$ were not determined independently, but were assumed to be proportional to the magnetic field, using the value which gave the best fit for the attenuation measurements at fixed magnetic field. This assumption is justified by the magnetoresistance measurements of Borovik and Volotskaya (1960).

The straight lines drawn on Figs. 8 and 9 show the theoretical dependence of ak_i on $1/\Omega\tau$, which is linear. The upper line is computed from the KMT theory and includes contributions to damping from currents on the surface of the sample as well as in its volume, while the lower line, computed with the boundary conditions $b_r = o$, does not include damping due to surface currents.

The object of plotting in this way is to show the effect of surface currents by extrapolating $1/\Omega\tau$ to zero (i.e. $\Omega\tau \to \infty$) so that there is no contribution to the damping from volume currents. The intercept on the vertical axis thus represents the damping due to surface currents.

In a third set of measurements, the sense of rotation of the m = 1 launching field relative to the steady axial magnetic field B_z was reversed by changing the phase difference between the launching coils from $\pi/2$ to $-\pi/2$, or by reversing B_z. It is important to realise that this is not equivalent to changing the polarisation of the wave, which is determined by the phase relation between b_r and b_θ. Changing the direction of rotation of the launching field relative to B_z reverses the direction of rotation of the whole field pattern, while retaining the same phase relation between b_r and b_θ. However, as discussed by KMT, only modes which have radial nodes can be propagated when m = -1. The measured dispersion relation and the damping for these m = -1 waves are shown in Figs. 10 and 11 on which are also plotted curves computed from the KMT theory. The mode having one radial node is designated m = -1, n = 2.

5. ACCURACY OF THE MEASUREMENTS

The main source of error in the determination of the dispersion relations was in the measurement of wavelengths and varied from about 1% at the high frequency end, where several wavelengths were included, to about 10% at the low frequency end, where only about one half wavelength could be included. The spread in each result was estimated from the maximum and minimum slopes of straight lines which could be drawn through the experimental points plotted on linear graph paper. The inhomogeneity of the magnetic field within the measuring volume was ±1%, but the effect of this on the overall accuracy was less at the higher frequencies because more wavelengths were included in a measurement. Errors due to other sources, namely determination of sample diameter, magnetic field and frequency, together amount to about 0.5%. Combining these errors, it is believed that the points at the high frequency ends of the dispersion relations have standard deviations of ±1.5%, the error increasing as the frequency decreases, as shown by the vertical bars in Figs. 4 6 and 10.

For the attenuation measurements, the accuracy was more uniform over the frequency range covered, but fell at the lower frequencies because of the increased attenuation. For the m = 1 experiments the errors increased at the higher frequencies because the pick-up coil dimensions became comparable with the wavelength. The spread in each result was estimated from the maximum and minimum slopes of straight lines which could be drawn through the experimental points plotted on semi-logarithmic graph paper. The detected signal was very sensitive to small inaccuracies of alignment etc. and the overall accuracy varies between about 5% and 10%, as shown by the vertical bars in Figs. 5 and 7.

The m = -1 measurements were more difficult because only a small amount of break-through of the less attenuated m = 1 mode could introduce spurious variations in amplitude and phase. The accuracy of these results is thus lower as shown in Figs. 10 and 11.

6. DISCUSSION OF RESULTS

Two conclusions can be drawn from a comparison of the experimental and computed dispersion relations for m = o and m = 1 (Figs. 4 and 6). The first is that the KMT theory, using rigorous boundary conditions and including surface currents, is verified within the experimental error for the range of conditions studied here, whereas if surface currents are excluded, discrepancies up to 70% are found. Secondly, using the exact boundary conditions, the experimental results agree with the dispersion relation computed with the assumption of one hole per atom. For each experimental point, a value can be found for the ratio of the experimental Hall coefficient at 15.4 kG and that calculated on the basis of one hole per atom. The weighted means of these ratios $R_H(\text{exp})/R_H(\text{calc})$ for all the points are: 0.992 ± 0.015 for m = o and 0.990 ± 0.015 for m = 1. These figures contrast with the work of Jones and Chambers (1962), where a discrepancy of about 5% was found between measured and calculated values of the high-field Hall coefficients in several metals; it is possible that the discrepancy in comparing their results with theory arose from the use of boundary conditions which did not take into account the vacuum field of the wave.

Considering the damping results shown in Figs. 5 and 7, the experiments provide further confirmation of the KMT theory. However, an unexplained feature of these results is the value of $\Omega\tau$ to give the best fit at 15.4 kilogauss. It is between 20 and 30 for the m = o mode and about 13 for the m = 1 mode. A possible explanation is that the attenuation due to surface currents may be different for different waves because of the physical conditions of the surface layer of the sample. Since the fractional contribution to the total damping due to surface currents is theoretically greater for the m = 1 mode than for

the m = o mode (see Figs. 5 and 7), such an effect would result in a lower effective $\Omega\tau$ for m = 1 than for m = o, as observed.

The effect of surface damping can be seen most clearly in Figs. 8 and 9 where, by extrapolating to $1/\Omega\tau = 0$, as explained in Section 4 above, the intercept on the vertical axis shows the effect of surface damping alone. Without surface damping, a straight line drawn through the points should pass through the origin, whereas it is found that even if a different value for the ratio $\Omega\tau/B$ is assumed, it is not possible to draw a line through the points and the origin.

Turning now to the m = -1 results, it is found that the experimental dispersion relation (Fig.10) differs from that computed for m = -1, n = 2 over the whole frequency range. On the other hand, the experimental damping results are in quite good agreement with the computations, if a value for $\Omega\tau$ at 15.4 kG of between 20 and 30 is assumed. It is clear from the trend shown by the calculated dispersion relations (see KMT, Fig.4), that these experimental results cannot be accounted for by taking higher modes into consideration. From the experimental data the possibility of these waves being a mixture of modes can be excluded. The rather unsatisfactory conclusion is, that these observations correspond to a mode not yet investigated theoretically. In an earlier experiment in which an attempt was made to launch the m = +1 wave by means of a single coil at the end of the sample, both m = +1 and m = -1 waves were launched simultaneously, amd gave rise to marked interference patterns between the two modes.

7. CONCLUSIONS

The agreement between the present experiments and the theory of KMT, apart from an isolated instance, allows three main conclusions to be drawn. Firstly, equation 1 is adequate to describe the properties of small amplitude electromagnetic fields in metals at low temperature, provided the wave frequencies considered are well below the Doppler shifted cyclotron frequency of the charges. Secondly, in applying boundary conditions at the interface between the metal and the surrounding vacuum, the wave fields in the vacuum associated with those in the metal must be taken into account. When this is done it is found that significant currents flow on the surface of the metal, which give rise to enhanced attenuation. This attenuation has been demonstrated experimentally. Thirdly, a comparison between the experimental and theoretical dependence of wavelength on frequency in a sample of known dimensions allows the Hall coefficient at 15.4 kG to be determined absolutely. The value found is consistant, within the experimental error (±1.5%) with that calculated assuming one hole per atom in indium.

8. ACKNOWLEDGEMENTS

The authors are grateful to B. McNamara who prepared the programme for the computations and arranged for them to be carried out; to J.P. Klozenberg for valuable discussions; and to D.G. Wood for constructing much of the apparatus and assisting with the experimental work.

9. REFERENCES

AIGRAIN, P., 1960, Proc. Int. Conf. on Semi-conductor Physics, Prague, p.224.

BOROVIK, E.S. and VOLOTSKAYA, V.G., 1960, J. Exptl. Theoret. Phys. USSR, 38, 261. (English translation Soviet Physics JETP 11, 189).

BOWERS, R., LEGENDY, C. and ROSE, F.E., 1961, Phys. Rev. Letters 7, 339.

COTTI, P., WYDER, P., and QUATTROPANI, A., 1962, Physics Letters 1, 50.

COTTI, P., WYDER, P., and QUATTROPANI, A., 1963, Phys. Kondens. Materie 1, 27.

DELLIS, A.N. and WEAVER, J.M., 1964, Proc. Phys. Soc., London, 83, 473.

GALLET, R.M., RICHARDSON, R.M., WEIDER, B., WARD, G.D. and HARDING, G.N., 1960, Phys. Rev. Letters 4, 347.

JONES, B.K. and CHAMBERS, R.G., 1962, Proc. Roy. Soc., London, A 270, 417.

KLOZENBERG, J.P., McNAMARA, B. and THONEMANN, P.C., 1964, Jnl. Fluid. Mech. (in press).

LIBCHABER, A. and VEILEX, R., 1962a, Phys. Rev., 127, 774.

LIBCHABER, A. and VEILEX, R., 1962b, Proc. Int. Conf. on Physics of Semiconductors, Exeter, p.138.

MERRILL, J.R., TAYLOR, M.T. and GOODMAN, J.M., 1963, Phys. Rev. 181, 2499.

ROSE, F.E., TAYLOR, M.T. and BOWERS, R., 1962, Phys. Rev. 127, 1122.

STOREY, L.R.O., 1953, Phil. Trans. Roy. Soc., A 246, 113.

SWENSON, C.A., 1955, Phys. Rev., 100, 1607.

TAYLOR, M.T., MERRILL, J.R. and BOWERS, R., 1963a, Phys. Rev., 129, 2525.

TAYLOR, M.T., MERRILL, J.R. and BOWERS, R., 1963b, Physics Letters 6, 159.

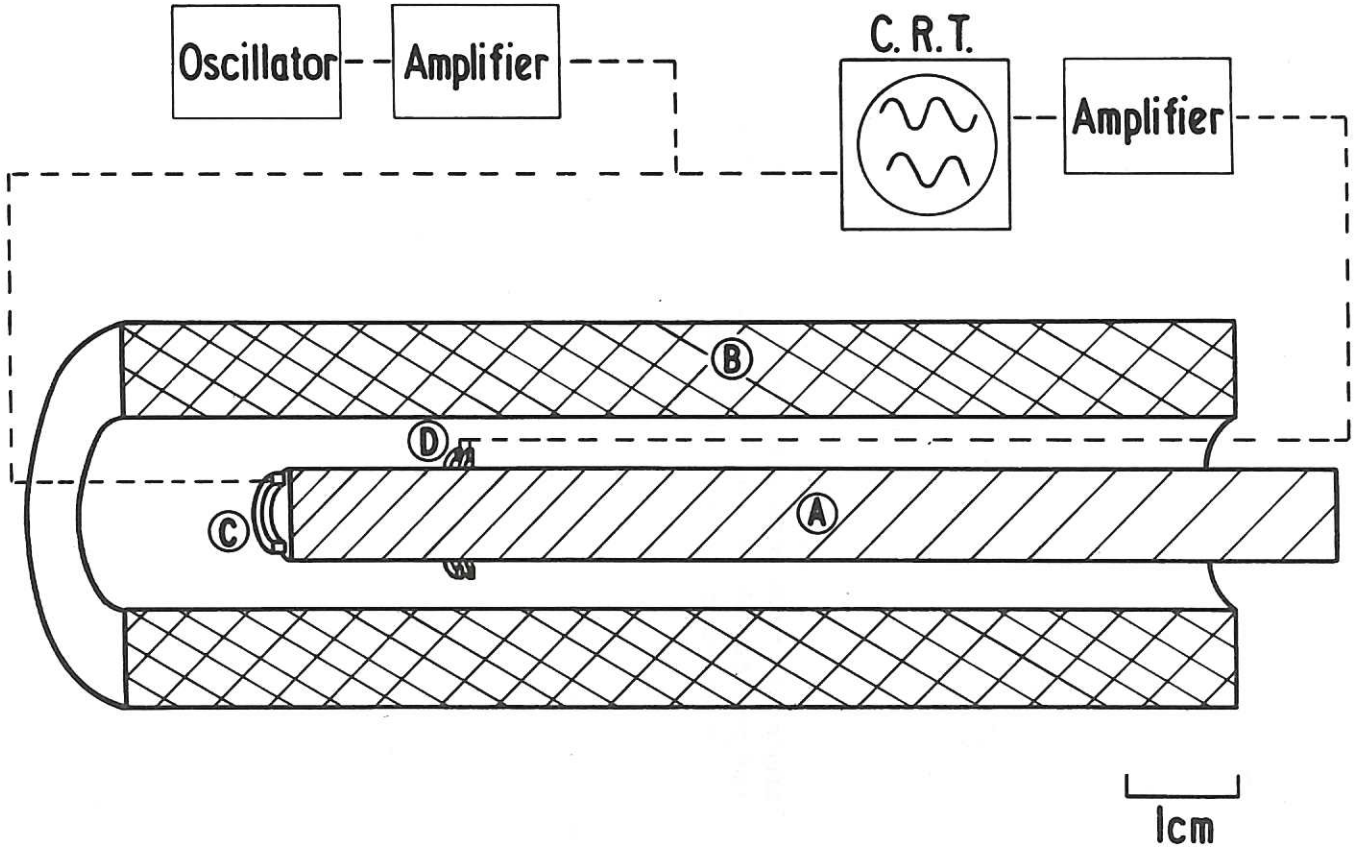

CLM-P 54 Fig. 1
Schematic diagram of experimental arrangement showing: A: Indium cylinder, B: Superconducting solenoid; C: Launching coil for m = 0 wave; D: Movable receiving coil

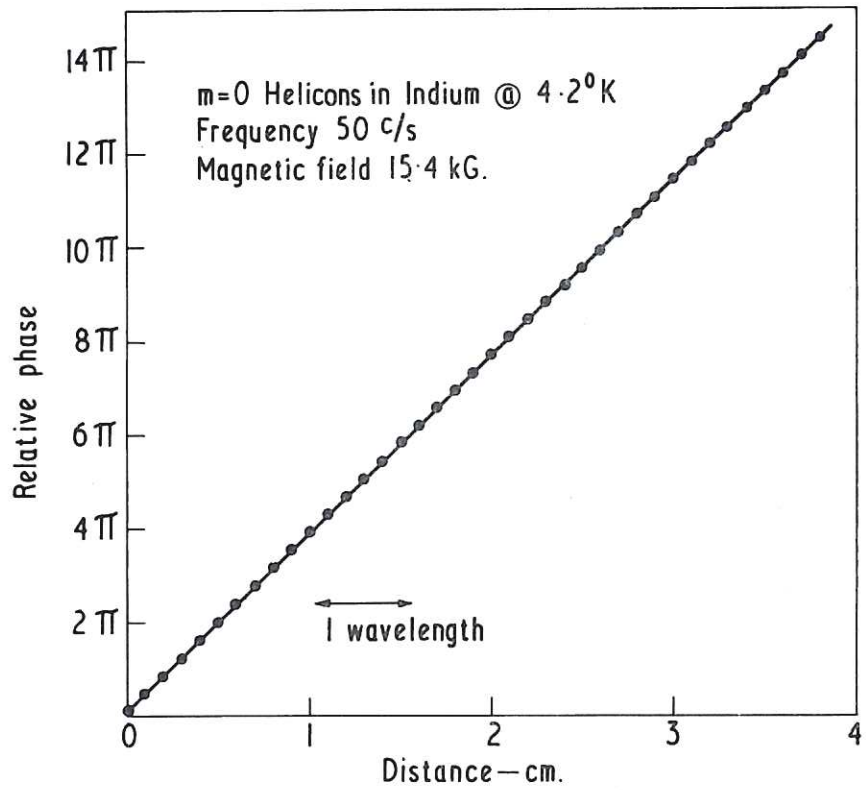

CLM-P 54 Fig. 2
Example of an experimental distance-phase measurement used to find the phase velocity of an m = 0 wave. The dimensions of the dots indicate the probable experimental error

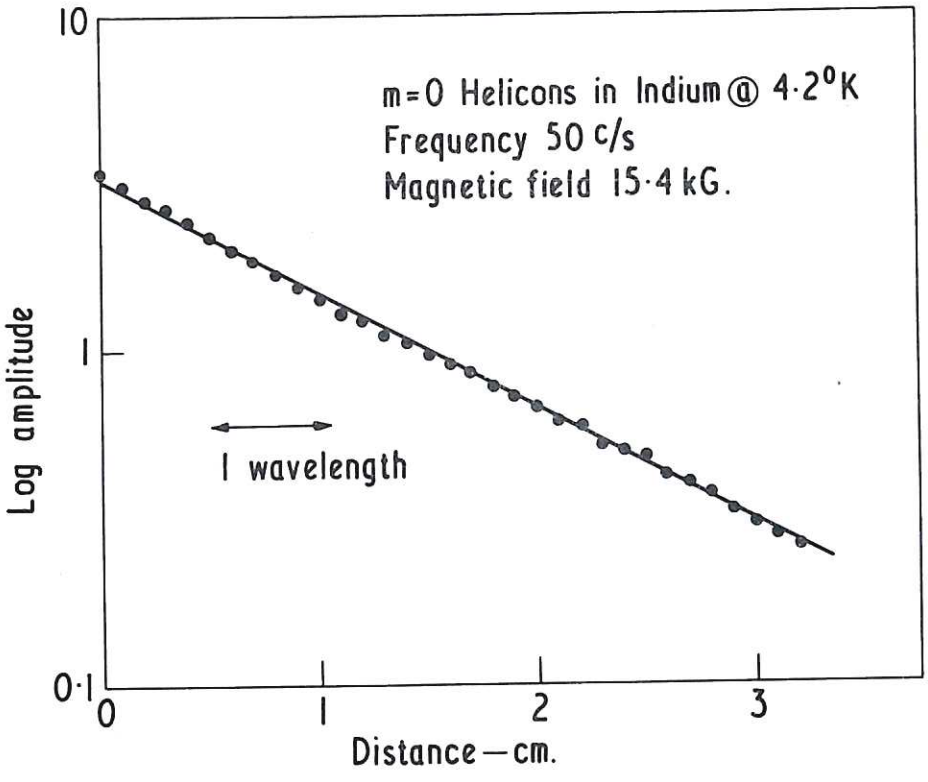

CLM-P 54 Fig. 3
Example of an experimental amplitude-distance measurement used to determine the attenuation of an m = 0 wave

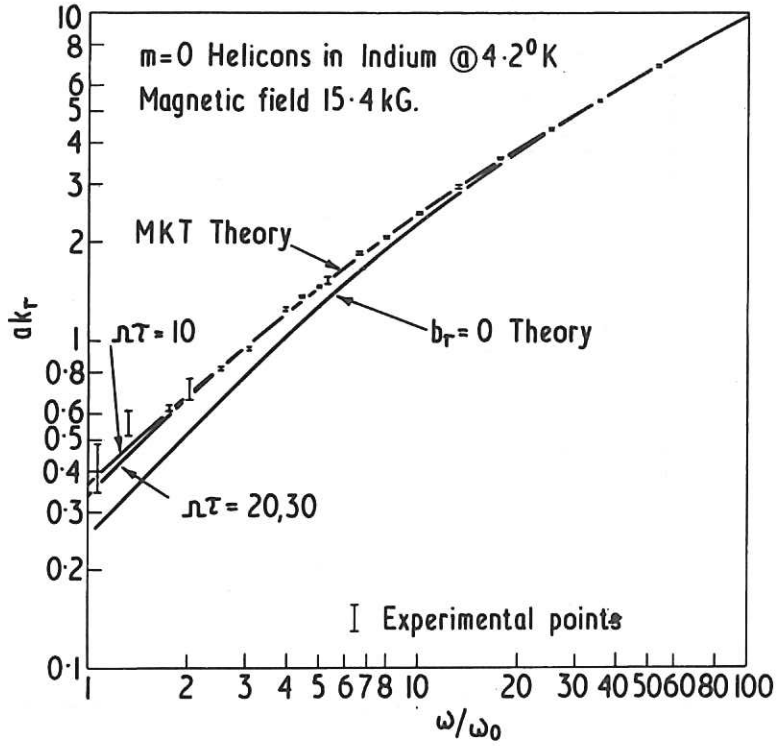

CLM-P 54 Fig. 4

Comparison of the experimentally determined wavelength-frequency results with theory for m = 0 helicons. Three theoretical curves are shown The uppermost curves, which are nearly coincident, are computed from the KMT theory for the values of $\Omega\tau$ shown. The lower curve, marked 'o_r = 0 theory' is the computed result ignoring vacuum fields and putting $\Omega\tau = \infty$. The lengths of the vertical bars indicate the experimental errors, estimated as described in the text

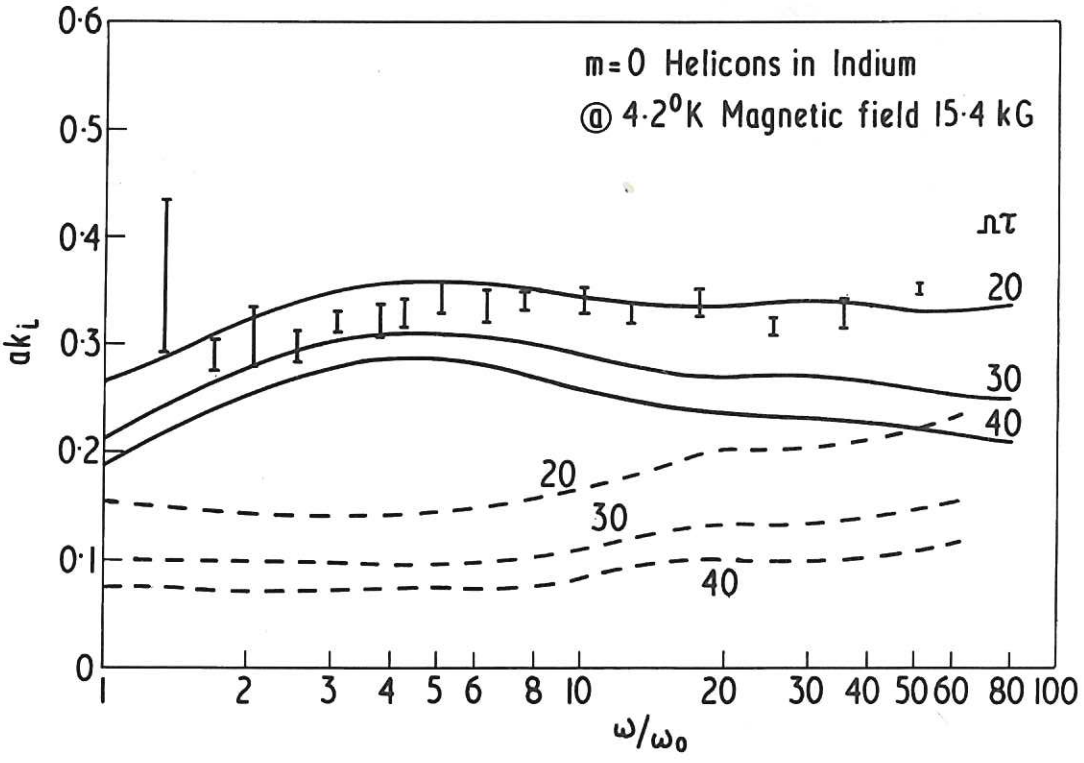

CLM-P 54 Fig. 5

Comparison of the experimentally determined attenuation of m = 0 helicons with theory. The dotted curves are calculated from theory with surface currents neglected, and the full curves with surface currents included, for three values of $\Omega\rho$. The lengths of the vertical bars indicate the experimental errors, estimated as described in the text

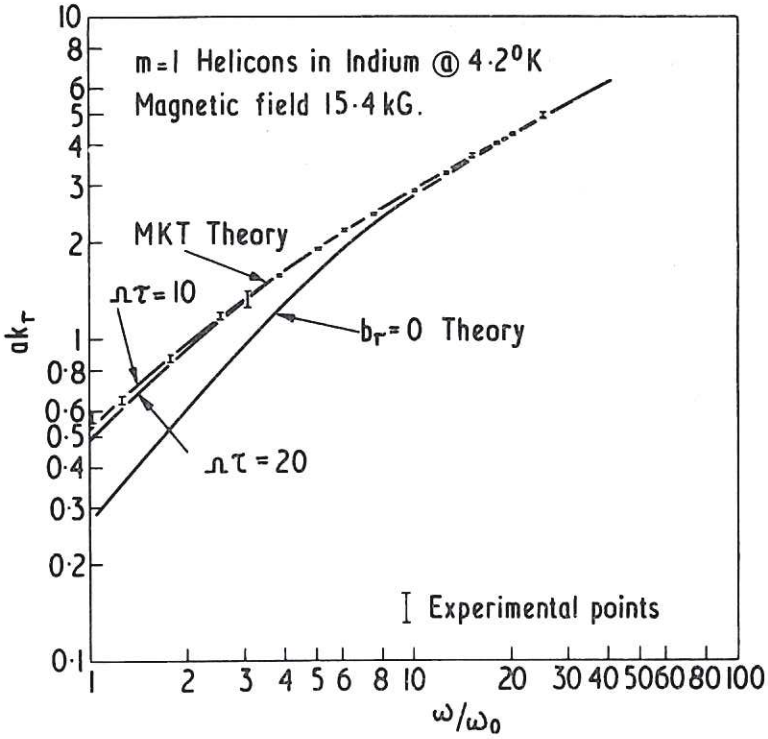

CLM-P 54 Fig. 6
Comparison of the experimentally determined wavelength-frequency results with theory for m = 1 helicons. For an explanation, see Fig. 4

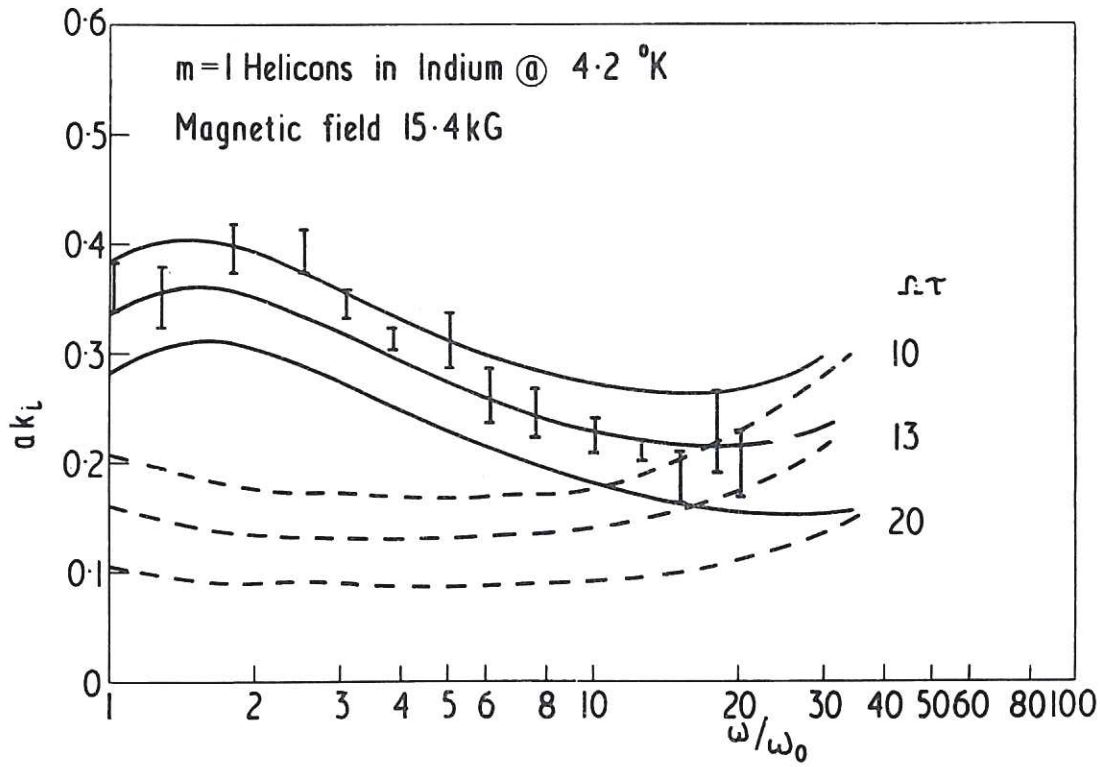

CLM-P 54 Fig. 7
Comparison of the experimentally determined attenuation of m = 1 helicons with theory. For an explanation, see Fig. 5

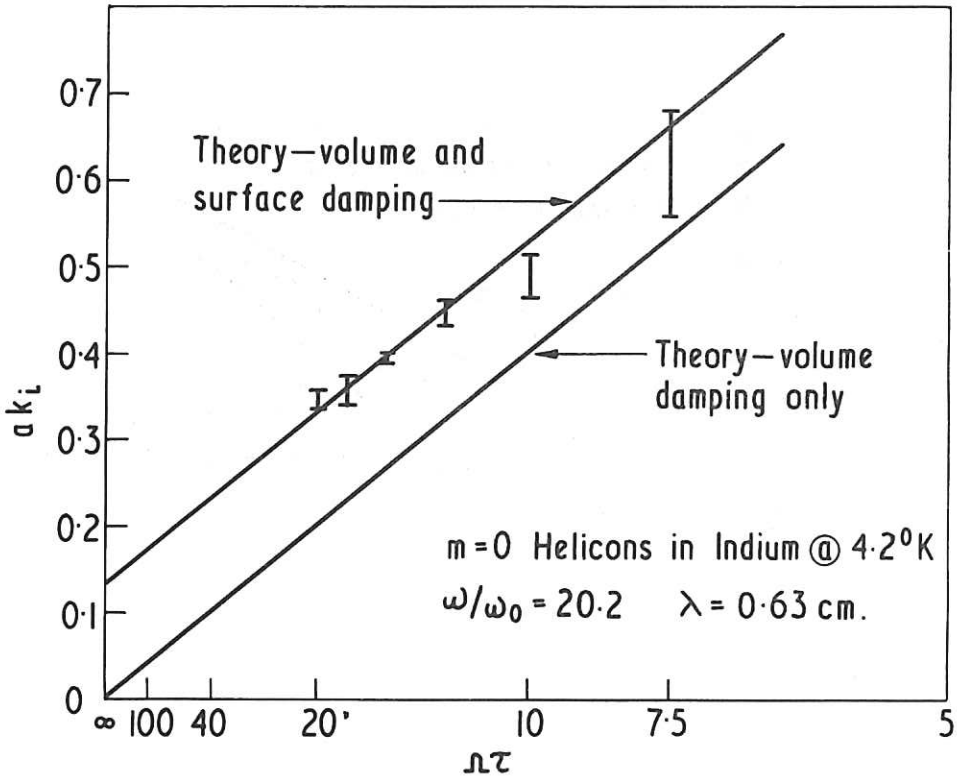

CLM-P54 Fig. 8

Comparison of the experimentally determined attenuation of m = 0 helicons with theory when the magnetic field and frequency were both varied in such a way that the wave-length remained constant. For the abscissae, the magnetic field has been converted into the appropriate value of $\Omega\tau$, in order to show the residual attenuation caused by surface currents as $\Omega\tau \to \infty$. The upper straight line is the theoretical result including surface currents, and the lower line the theoretical result neglecting surface currents

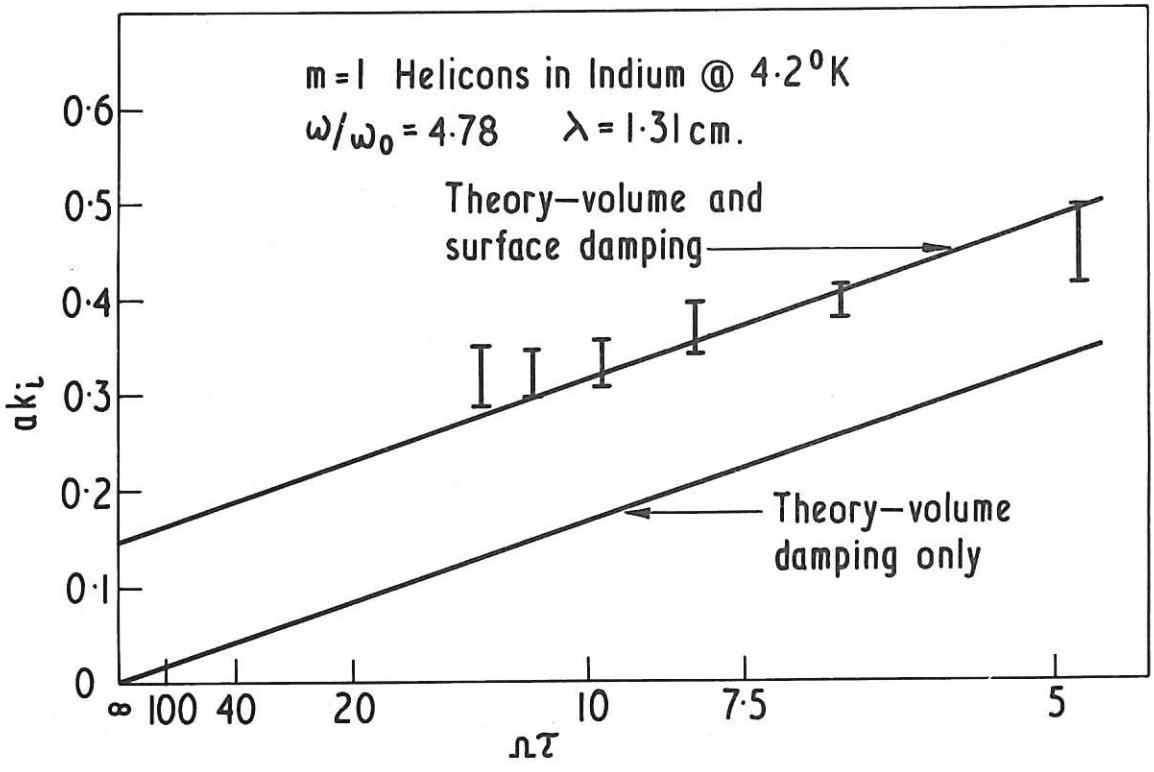

CLM-P54 Fig. 9

Comparison of the experimentally determined attenuation of m = 1 helicons with theory. For an explanation, see Fig. 8

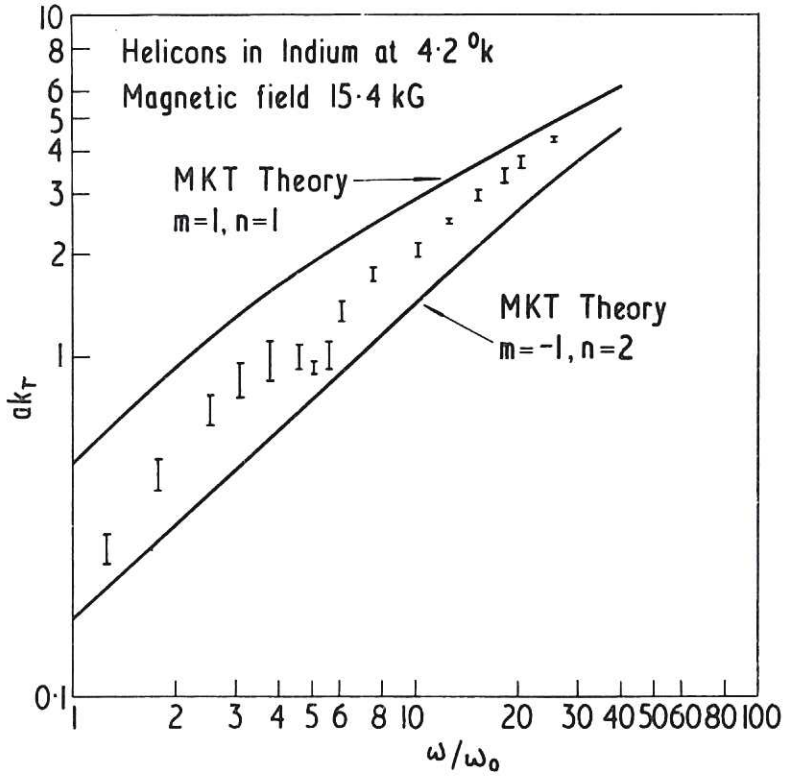

CLM-P 54 Fig. 10

Comparison with theory of the experimentally determined wavelength-frequency results obtained by reversing the direction of rotation of the magnetic field pattern of the launching coil compared to the direction used to obtain Fig. 6. The upper full curve is computed from the KMT theory for the mode m = 1, n = 1; the lower for m = – 1, n = 2

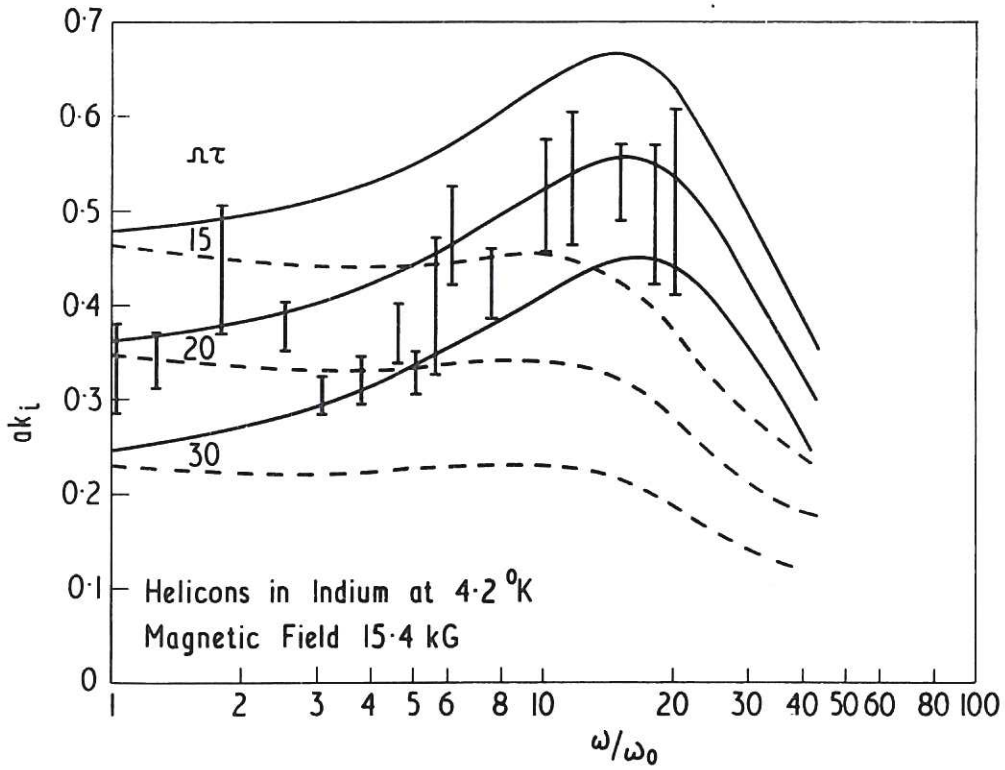

CLM-P 54 Fig. 11

Comparison with theory of the experimentally determined wavelength-frequency results obtained by reversing the direction of rotation of the magnetic field pattern of the launching coil compared to the direction used to obtain Fig. 7. For an explanation, see Fig. 5